Available online at www.sciencedirect.com
ScienceDirect
Journal of Organometallic Chemistry 693 (2008) 1787–1796
Journal of Organometallic Chemistry
www.elsevier.com/locate/jorganchem

Syntheses, X-ray structures and CVD studies of diorganoalkoxogallanes

Siama Basharat [a], Claire J. Carmalt [a,*], Robert Palgrave [a], Sarah A. Barnett [a], Derek A. Tocher [a], Hywel O. Davies [b]

[a] *Materials Chemistry Centre, Department of Chemistry, University College London, 20 Gordon Street, London WC1H 0AJ, UK*
[b] *SAFC Hitech, Power Road, Bromborough, Wirral CH62 3QF, UK*

Received 19 December 2007; received in revised form 24 January 2008; accepted 24 January 2008
Available online 2 February 2008

Abstract

Structural studies by X-ray crystallography have been carried out for a range of diorganoalkoxogallanes incorporating donor-functionalized ligands. The compounds $[Et_2Ga(\mu\text{-}OR)]_2$ (**1**, $R = CH_2CH_2NMe_2$; **2**, $R = CH(CH_3)CH_2NMe_2$; **3**, $C(CH_3)_2CH_2OMe$; **4**, $R = CH(CH_2NMe_2)_2$) adopt dimeric structures with a planar Ga_2O_2 ring, and each gallium atom is coordinated in a distorted trigonal bipyramidal geometry. Low pressure chemical vapor deposition (CVD) of **2** and **4** resulted in the formation of oxygen deficient gallium oxide thin films on glass. However, the reaction of Et_3Ga and ROH ($R = CH_2CH_2NMe_2$, $CH(CH_3)CH_2NMe_2$, $C(CH_3)_2CH_2OMe$, $CH(CH_2NMe_2)_2$) in toluene under aerosol assisted (AA)CVD conditions afforded stoichiometric Ga_2O_3 thin films on glass. This CVD technique offers a rapid, convenient route to Ga_2O_3, which involves the *in situ* formation of diethylalkoxogallanes, of the type $[Et_2Ga(\mu\text{-}OR)]_2$, the structures of which are described in this paper. The gallium oxide films were deposited at 450 °C and analyzed by scanning electron microscopy (SEM), X-ray powder diffraction, wavelength dispersive analysis of X-rays (WDX), X-ray photoelectron spectroscopy (XPS) and Raman spectroscopy.

Keywords: Gallium alkoxide; Chemical vapour deposition; Thermal decomposition

1. Introduction

Gallium oxide thin films are attractive materials for use as gas sensors at high temperatures [1–4]. It has been reported as having a response to oxidizing gases at elevated temperatures (>900 °C) [5] and a response to reducing gases at lower temperatures (500 °C) [6]. Gallium oxide (Ga_2O_3) is a wide band gap semiconductor material, which has also received attention as a compound semiconductor passivator [7] and as a luminescent phosphor [8–10].

Thin films of Ga_2O_3 have been prepared in a variety of ways. Physical vapor deposition methods have been employed, for example electron-beam evaporation and magnetron sputtering [11,12]. Atmospheric pressure chemical vapor deposition (CVD) of $GaCl_3$ and methanol [13] and low pressure CVD of homoleptic gallium alkoxides [14], gallium tris-hexafluoroacetylacetonate [15], gallium fluoroalkoxide [16] and gallium sesquialkoxide [17] has also been conducted. However, none of these precursors are entirely satisfactory, for example the presence of fluorinated ligands can result in fluorine contamination, which could induce problems for gas sensor applications, due to changes in baseline resistance and sensor drift. Nonetheless, the production of thin films by CVD results in inexpensive, reproducible and adhesive films with low-impurity levels and may therefore provide an advantageous method of producing gas sensors if a suitable precursor can be designed.

We have recently been investigating the synthesis of gallium [18] and indium [19] alkoxides [20] incorporating donor-functionalized ligands. These ligands were chosen for CVD, as they lead to precursors, which are less air/moisture sensitive and have increased solubility [21]. The high moisture sensitivity of dialkylalkoxogallanes makes them difficult to use in solution-based CVD.

* Corresponding author. Tel.: +44 (0)207 679 7528; fax: +44 (0)207 679 7463.
E-mail address: c.j.carmalt@ucl.ac.uk (C.J. Carmalt).

0022-328X/$ - see front matter © 2008 Elsevier B.V. All rights reserved.
doi:10.1016/j.jorganchem.2008.01.042

However, the modified alkoxides with donor-functionalized ligands ($OCH_2CH_2NMe_2$, $CH(CH_3)CH_2NMe_2$, etc.) have an increased coordinative saturation at the metal center and so provide stability. Furthermore, the aminoalkoxide ligand eliminates the necessity of introducing an extra donor group to stabilize the electron deficient gallium alkoxide complex. In this report, structural studies on diethylalkoxogallanes, of the type $[Et_2Ga(\mu\text{-}OR)]_2$, prepared from the solution phase reaction of Et_3Ga and ROH, are described. Low pressure CVD employing selected precursors is also reported. In addition, thin film growth of gallium oxide by a novel aerosol assisted (AA)CVD route from the reaction of Et_3Ga and donor-functionalized alcohols is described. Different and unique morphologies of films can be obtained by AACVD due to the influence of the solvent on the deposition, which could potentially lead to improved properties. Furthermore, thin films can be deposited under AACVD conditions at low temperatures and require only minimal amounts of precursor (*ca.* 0.1 g). In this study, gallium alkoxides were generated *in situ* from the reaction of Et_3Ga and ROH (R = $CH_2CH_2NMe_2$, $CH(CH_3)CH_2NMe_2$, $C(CH_3)_2CH_2OMe$, $CH(CH_2NMe_2)_2$) in toluene. An aerosol of this reaction mixture was then passed over a heated glass substrate, which resulted in the deposition of thin films of gallium oxide.

2. Experimental

2.1. General procedures for synthesis

All manipulations were performed under a dry, oxygen-free dinitrogen atmosphere using standard Schlenk techniques or in an Mbraun Unilab glovebox. All solvents used were stored in alumina columns and dried with anhydrous engineering equipment, such that the water concentration was 5–10 ppm. Compounds **1**–**4** were prepared using modified literature procedures [17]. SAFC HiTech supplied triethylgallium. All other reagents were procured commercially from Aldrich and the alcohols were degassed by three freeze–pump–thaw cycles and stored over 4 Å molecular sieves. Microanalytical data were obtained at University College London.

All ^1H and ^{13}C NMR spectra were obtained on a Bruker AMX400 spectrometer, operating at 400.12 MHz. All spectra were recorded using C_6D_6, which was dried and degassed over molecular sieves prior to use; ^1H and ^{13}C chemical shifts are reported relative to $SiMe_4$ (δ 0.00). All IR spectra were recorded using a Shimadzu FTIR-8200 spectrometer, operating in the region of 4000–400 cm^{-1}. The IR samples were prepared using nujol. The mass spectra were obtained using a Micromass 70-SE spectrometer using Chemical Ionization (CI) with methane reagent gas.

2.2. General conditions for AACVD

Nitrogen (99.99%) was obtained from BOC and used as supplied. Depositions were obtained on SiCO coated float-glass. Prior to use the glass substrates were cleaned using petroleum ether (60–80 °C) and propan-2-ol and then dried in air. Glass substrates of *ca.* 90 mm × 45 mm × 4 mm were used. The precursor was dissolved in solvent and vaporized at room temperature by use of a PIFCO ultrasonic humidifier, producing an aerosol of the precursor in toluene. Two-way taps were used to divert the nitrogen carrier gas through the bubbler and the aerosol was carried into the reactor in a stream of nitrogen gas through a brass baffle to obtain a laminar flow.

A graphite block containing a Whatman cartridge heater was used to heat the glass substrate. The temperature of the substrate was monitored by a Pt–Rh thermocouple. Depositions were carried out by heating the horizontal bed reactor to the required temperature before diverting the nitrogen line through the aerosol and hence to the reactor. The total time for the deposition process was in the region of 2–3 h. At the end of the deposition the nitrogen flow through the aerosol was diverted and only nitrogen passed over the substrate. The glass substrate was allowed to cool with the graphite block to less than 100 °C before it was removed. Coated substrates were handled and stored in air. Large pieces of glass (*ca.* 4 cm × 2 cm) were used for X-ray powder diffraction. The coated glass substrate was cut into *ca.* 1 cm × 1 cm squares for subsequent analysis by scanning electron microscopy (SEM), wavelength dispersive analysis of X-rays (WDX), X-ray photoelectron spectroscopy (XPS), transmission/reflectance and UV absorption studies.

2.3. Film analysis methods

X-ray powder diffraction patterns were measured on a Siemens D5000 diffractometer using monochromated Cu Kα1 radiation (λ = 1.5400 Å) radiation. The diffractometer used glancing incident radiation (1.5°). The films on the glass substrates were indexed using Unit Cell and compared to database standards. Raman spectra were acquired using a Renishaw Raman system 1000 using a helium–neon laser of wavelength 632.8 nm. The Raman system was calibrated against the emission lines of neon. SEM was carried out on a JEOL 6301 filament scanning electron microscope and WDX was obtained on a Philips XL30SEM instrument. X-ray photoelectron spectra were recorded using a VG ESCALAB 220i XL instrument using focused (300 μm spot) monochromatic Al Kα radiation at a pass energy of 20 eV. Scans were acquired with steps of 50 meV. A flood gun was used to control charging and binding energies were referred to an adventitious C 1s peak at 285.0 eV. Reflectance and transmission spectra were recorded between 300 and 1000 nm by a Zeiss miniature spectrometer. Reflectance measurements were standardized relative to a rhodium mirror and transmission relative to air. UV–Vis spectra were recorded using a Helios double beam instrument between 200 and 1000 nm.

2.4. Synthesis of diorganoalkoxygallanes

2.4.1. $[Et_2Ga(OCH_2CH_2NMe_2)]_2$ (1)

$HOCH_2CH_2NMe_2$ (0.68 mL, 6.75 mmol) was added dropwise to a solution of Et_3Ga (1.00 mL, 6.75 mmol) in toluene (20 mL) at −78 °C with stirring over a 0.5 h period. The reaction mixture was allowed to warm slowly to room temperature and stirred for a further 24 h. Removal of the solvent *in vacuo* afforded a colorless oil. The reaction flask was left at room temperature and X-ray quality single crystals were obtained after several days (1.38 g, yield 95%). Anal. Calc. for $C_8H_{20}NOGa$: C, 44.49; H, 9.33; N, 6.49. Found: C, 44.48; H, 9.32; N, 6.91%. ^{1}H NMR δ/ppm (C_6D_6): 0.44 (quartet, $GaCH_2CH_3$, 4H, $J = 8.1$ Hz), 1.29 (t, $GaCH_2CH_3$, 6H, $J = 8.1$ Hz), 1.98 (s, NCH_3, 6H), 2.01 (t, OCH_2CH_2N, 2H, $J = 8.0$ Hz), 3.49 (t, OCH_2CH_2N, 2 H, $J = 8.1$ Hz). $^{13}C\{^1H\}$ NMR δ/ppm (C_6D_6): 4.1 ($GaCH_2CH_3$), 11.0 ($GaCH_2CH_3$), 45.2 (NCH_3), 59.1 (OCH_2CH_2N), 61.7 (OCH_2). IR (cm^{-1}): 2924 vs, 2789 w, 2719 w, 2700 w, 1666 s, 1420 m, 1356 m, 1273 s, 1233 w, 1187 m, 1165 w, 1036 m, 1000 m, 954 m, 932 m, 894 m, 786 m, 629 m, 552 m, 504 m, 430 m. Mass spec. (CI): (*m*/*z*) 433 ([M]), 403 ([M]–Et), 344 ([M]–($OCH_2CH_2NMe_2$)), 216 ($Et_2Ga(OCH_2CH_2NMe_2)$), 186 ($EtGa(OCH_2CH_2NMe_2)$), 127 (Et_2Ga).

2.4.2. $[Et_2Ga(OCH(CH_3)CH_2NMe_2)]_2$ (2)

Compound **2** was prepared in the same manner as **1** using $HOCH(CH_3)CH_2NMe_2$ (0.83 mL, 6.74 mmol) and Et_3Ga (1.00 mL, 6.75 mmol). Removal of the solvent *in vacuo* afforded a yellow non-viscous oil. The reaction flask was left at room temperature and X-ray quality single crystals were obtained after several days (1.42 g, yield 92%). Anal. Calc. for $C_9H_{22}NOGa$: C, 46.99; H, 9.64; N, 6.09. Found: C, 46.77; H, 9.28; N, 5.99%. ^{1}H NMR δ/ppm (C_6D_6): 0.56 (quartet, $GaCH_2CH_3$, 4H, $J = 8.0$ Hz), 1.39 (t, $GaCH_2CH_3$, 6 H, $J = 8.0$ Hz), 1.56 (d, $OCH(CH_3)CH_2$, 3H, $J = 6.10$ Hz), 1.90 (s, NCH_3, 6H), 2.08 (m, $OCHCH_2N$, 2H, 11.1 Hz), 3.81 (m, $OCH(CH_3)CH_2$, 1H). $^{13}C\{^1H\}$ NMR δ/ppm (C_6D_6): 6.36 ($GaCH_2CH_3$), 11.6 ($GaCH_2CH_3$), 23.0 ($GaOCH(CH_3)$), 46.4 (NCH_3), 65.4 ($OCHCH_2N$), 69.5 ($GaOCH$). IR (cm^{-1}): 2926 vs, 2723 m, 1687 w, 1421 m, 1342 m, 1316 m, 1260 m, 1279 m, 1198 m, 1140 m, 1032 s, 947 s, 865 m, 837 m, 662 m, 619 m, 553 m, 519 m, 422 m. Mass spec. (CI): (*m*/*z*) 461 ([M]), 431 ([M]–Et), 358 ([M]–$OCH(CH_3)CH_2NMe_2$), 230 ($Et_2GaOCH(CH_3)CH_2NMe_2$), 200 ($EtGa(OCH(CH_3)CH_2NMe_2)$), 127 (Et_2Ga).

2.4.3. $[Et_2Ga(OC(CH_3)_2CH_2OMe)]_2$ (3)

Compound **3** was prepared in the same way as **1** using $HOC(CH_3)_2CH_2OMe$ (0.79 mL, 6.75 mmol) and Et_3Ga (1.00 mL, 6.75 mmol). Removal of the solvent *in vacuo* afforded a caked white solid. The solid was redissolved in toluene (2 mL) and cooled to −20 °C. Compound **3** was obtained as colorless crystals after several days (1.50 g, yield 96%). Anal. Calc. for $C_9H_{21}O_2Ga$: C, 46.80; H, 9.16. Found: C, 46.26; H, 9.29%. ^{1}H NMR δ/ppm (C_6D_6): 0.64 (quartet, $GaCH_2CH_3$, 4H, $J = 8.1$ Hz), 1.23 (s, $GaOC(CH_3)$, 6H), 1.40 (t, $GaCH_2CH_3$, 6H, $J = 8.1$ Hz), 2.88 (s, $GaOCCH_2$, 2H), 3.03 (s, OMe, 3H). $^{13}C\{^1H\}$ NMR δ/ppm (C_6D_6): 8.1 ($GaCH_2CH_3$), 10.5 ($GaCH_2CH_3$), 27.4 ($OC(CH_3)$), 58.4 (OCH_3), 72.6 ($OCCH_2$), 81.9 ($OCCH_2$). IR (cm^{-1}): 2923 vs, 2726 w, 1565 w, 1463 s, 1364 m, 1238 m, 1178 m, 1152 m, 1112 m, 1002 m, 961 m, 936 m, 918 m, 796 m, 658 m, 633 m, 556 m. Mass spec. (CI): (*m*/*z*) 433 ([M]–Et), 358 ([M]–($OC(CH_3)_2CH_2OCH_3$)), 231 ($Et_2GaOC(CH_3)_2CH_2OCH_3$), 201 ($EtGaOC(CH_3)_2CH_2OCH_3$), 127 ($Et_2Ga$).

2.4.4. $[Et_2Ga(OCH(CH_2NMe_2)_2)]_2$ (4)

Compound **4** was prepared in the same manner as **1** using $HOCH(CH_2NMe_2)_2$ (1.10 mL, 6.75 mmol) and Et_3Ga (1.00 mL, 6.75 mmol). Removal of the solvent *in vacuo* afforded a yellow non-viscous oil. The reaction flask was left at room temperature and X-ray quality single crystals were obtained after several days (1.64 g, yield 89%). Anal. Calc. for $C_{11}H_{27}ON_2Ga$: C, 48.38; H, 9.97; N, 10.26. Found: C, 48.37; H, 9.97; N, 10.63%. ^{1}H NMR δ/ppm (C_6D_6): 0.58 (quartet, $GaCH_2CH_3$, 4 H, $J = 8.1$ Hz), 1.41 (t, $GaCH_2CH_3$, 6H, $J = 8.1$ Hz), 2.04 (s, NCH_3, 12H), 2.08 (m, $OCHCH_2N$, 4H), 3.81 (m, OCH, 1H). $^{13}C\{^1H\}$ NMR δ/ppm (C_6D_6): 5.0 ($GaCH_2CH_3$), 10.8 ($GaCH_2CH_3$), 46.2 (NCH_3), 66.7 ($OCHCH_2N$), 67.9 (OCH). IR (cm^{-1}): 3126 vs, 2927 vs, 2859 m, 2818 s, 2768 w, 2194 vs, 1323 s, 1262 vs, 1206 m, 1169 m, 1099 vs, 1033 vs, 959 w, 931 m, 901 m, 875 m, 855 w, 833 w, 820 w, 611 m, 615 m. Mass spec. (CI): (*m*/*z*) 401 ([M]–($OCH(CH_2NMe_2)_2$)), 243 ($Et_2Ga(OCH(CH_2NMe_2)_2)$), 127 (Et_2Ga).

2.5. Chemical vapour deposition studies

2.5.1. Low pressure CVD of 2

Compound **2** (0.3 g) was loaded into the sealed end of a quartz tube (500 mm length × 25 mm diameter) in the glovebox. Glass (70 mm × 6 mm × 2 mm) substrates were placed carefully along the inside of the tube. The tube was then placed in a furnace such that 35 cm was inside the furnace and the end containing the sample protruded by 5 cm. The tube was heated to a temperature of 600 °C under dynamic vacuum (3.0 kPa). The tube was slowly drawn into the furnace, *ca.* 1 cm/30 min until the sample started to melt. Once the compound had decomposed the furnace was allowed to cool to room temperature. Translucent light-grey films were deposited on the glass substrates. Low pressure CVD of compound **4** was also carried using the method described for precursor **2**.

2.5.2. AACVD reaction of Et_3Ga and $HOCH_2CH_2NMe_2$

$HOCH_2CH_2NMe_2$ (4.00 mL, 40.5 mmol) was placed in 30 mL of toluene in the AACVD bubbler and used to

pre-treat the reactor for 5 min before the addition of Et_3Ga. After pre-treating the reactor, Et_3Ga (1.00 mL, 6.75 mmol) was added to the bubbler. The mixture was allowed to react for 60 min prior to deposition.

2.5.3. AACVD reaction of Et_3Ga and $HOCH(CH_3)CH_2NMe_2$

The procedure was the same as above but using $HOCH(CH_3)CH_2NMe_2$ (5.00 mL, 40.5 mmol).

2.5.4. AACVD reaction of Et_3Ga and $HOC(CH_3)_2CH_2OMe$

The procedure was the same as above but using $HOC(CH_3)_2CH_2OMe$ (4.70 mL, 40.5 mmol).

2.5.5. AACVD reaction of Et_3Ga and $HOCH(CH_2NMe_2)_2$

The procedure was the same as above but using $HOCH(CH_2NMe_2)_2$ (6.60 mL, 40.5 mmol).

2.6. Crystal structures determination and refinement

Crystals of **3** were isolated from toluene at −20 °C; crystals of **1**, **2** and **4** were obtained from oils at room temperature after a few days. A single crystal was mounted on a glass fibre and all geometric and intensity data were taken from this sample on a Bruker SMART APEX CCD diffractometer using graphite-monochromated Mo Kα radiation ($\lambda = 0.71073$ Å) at 150 ± 2 K. Data reduction and integration was carried out with SAINT+ [22] and absorption corrections applied using the programme SADABS [23]. The structure was solved by direct methods using SHELXS-97 [24] and developed using alternating cycles of least-squares refinement and difference-Fourier synthesis [25]. For complexes **1**–**3**, all non-hydrogen atoms were refined anisotropically and hydrogen atoms were placed in calculated positions with their thermal parameters linked to those of the atoms to which they were attached (riding model). For complex **4**, the ligand was found to be partly disordered over two sites in the ratio 55:45. Some atomic positions were common to both parts (N1, N2, C4) and modeled anisotropically on one site while the others (C1–C7) were modeled anisotropically over two sites. The hydrogen atoms were geometrically placed on all atoms as necessary and treated as riding. Crystallographic refinement parameters of complexes **1**–**4** are summarized in Table 1, and the selected bond distances and angles of these complexes are listed in Table 2, respectively.

3. Results and discussion

3.1. Synthesis and characterization of diorganoalkoxygallanes

In a typical synthesis, the donor-functionalized alcohol was added to Et_3Ga in toluene, resulting in a violent evolution of ethane gas (Scheme 1). After work up, oils (**1**, **2** and **4**) or a white solid (**3**) resulted from which, colorless crystals of compounds **1**–**4** suitable for single crystal X-ray diffraction were afforded in 89–96% yields. Analytical and spectroscopic data for **1**–**4** indicated that the expected dimeric complexes $[Et_2Ga(\mu\text{-}OR)]_2$ ($R = CH_2CH_2NMe_2$ (**1**), $CH(CH_3)CH_2NMe_2$ (**2**), $C(CH_3)_2CH_2OMe$ (**3**) and $CH(CH_2NMe_2)_2$ (**4**)) had been isolated [18].

The dimeric nature of **1**–**4** was confirmed by single crystal X-ray crystallography (Figs. 1–4) and selected bond lengths and angles are given in Table 2. The four-membered Ga_2O_2 ring, that is common to this type of complex [20], is planar in **1**–**4**. Each gallium atom in **1**–**4** adopts a distorted trigonal bipyramidal geometry with two ethyl groups in equatorial positions. The bridging alkoxide groups are located in both axial and equatorial positions, while the donor atom (L) of the alkoxide ligand (N for **1**,

Table 1
Crystallographic data for compounds **1**–**4**

Data	**1**	**2**	**3**	**4**
Chemical formula	$C_{16}H_{40}Ga_2N_2O_2$	$C_{18}H_{44}Ga_2N_2O_2$	$C_{18}H_{42}Ga_2O_4$	$C_{22}H_{54}Ga_2N_4O_2$
Formula weight	431.94	459.99	461.96	546.13
T (K)	150(2)	150(2)	150(2)	150(2)
Crystal system	Monoclinic	Triclinic	Triclinic	Triclinic
Space group	$P2_1/n$	$P\bar{1}$	$P\bar{1}$	$P\bar{1}$
a (Å)	10.0583(7)	8.4541(10)	8.0695(8)	8.5041(8)
b (Å)	15.4421(11)	8.7564(11)	8.8229(9)	8.9640(9)
c (Å)	13.6263(10)	16.944(2)	8.8587(9)	9.9568(10)
α (°)	90	77.893(2)	108.355(2)	77.0570(10)
β (°)	90.5620(10)	80.226(2)	105.923(2)	83.2580(10)
γ (°)	90	73.674(2)	95.997(2)	82.2180(10)
V (Å^3)	2116.4(3)	1168.7(2)	562.92(10)	729.93(12)
Z	4	2	1	1
ρ_{calc} (g cm^{-3})	1.356	1.307	1.363	1.242
Reflections collected	18939	9984	4944	6419
Unique reflections (R_{int})	5074 (0.0186)	5297 (0.0282)	2583 (0.0116)	3346 (0.0118)
μ (mm^{-1})	2.554	2.317	2.409	1.867
R_1 [$F^2 > 2\sigma$]	0.0213	0.0417	0.0184	0.0260
wR_2 [all data]	0.0531	0.1097	0.0465	0.0696

Table 2
Selected bond lengths (Å) and angles (°) for complexes **1**–**4**

Compound	**1**	**2**		**3** [c]	**4** [d]
		Molecule A [a]	Molecule B [b]		
Ga–O	1.9229(10) 1.9337(9)	1.919(2)	1.920(2)	1.9299(9)	1.9149(11)
Ga–O′	2.0669(9) 2.0910(9)	2.088(2)	2.074(2)	2.0141(9)	2.0964(11)
Ga–L[a]	2.5068(12) 2.3727(11)	2.552(3)	2.600(3)	2.6266(10)	2.5256(16)
Ga–C	1.9843(14) 1.9786(14) 1.9848(14) 1.9856(14)	1.982(3) 1.978(3)	1.982(3) 1.974(3)	1.9748(13) 1.9737(10)	1.9731(19) 1.9758(19)
O–Ga–O′	74.48(4) 73.70(4)	75.07(10)	75.63(10)	77.27(4)	74.81(5)
O–Ga–C	117.84(5) 116.47(5) 116.82(5) 119.24(5)	115.78(12) 116.77(12)	115.46(12) 114.93(13)	113.59(5) 116.04(4)	118.28(7) 114.54(7)
O′–Ga–C	100.90(5) 98.58(5) 100.89(5) 97.00(5)	100.72(12) 98.38(12)	100.39(12) 99.51(13)	105.70(5) 106.74(5)	100.40(7) 97.90(7)
C–Ga–C	125.35(6) 123.86(6)	127.04(14)	128.90(15)	125.06(5)	126.90(9)
L–Ga–C	91.12(5) 96.84(5) 94.42(5) 96.43(5)	92.81(12) 93.56(12)	91.13(13) 93.58(14)	86.98(5) 87.77(5)	92.71(8) 94.41(8)
O–Ga–L	75.24(4) 75.45(4)	75.93(9)	75.29(9)	71.16(3)	76.36(5)
O′–Ga–L	149.63(4) 149.11(4)	150.98(9)	150.90(10)	148.43(3)	151.17(5)
Ga–O–Ga	105.50(4) 106.04(4)	104.93(10)	104.37(10)	102.73(4)	105.19(5)

Symmetry codes for O′: [a] $-x+1, -y+2, -z+1$; [b] $-x, -y+1, -z+2$; [c] $-x, -y+1, -z+1$; [d] $-x+1, -y+1, -z+1$.
[a] L = N for **1**, **2** and **4**; L = O for **3**.

2 and **4**; O for **3**) is in the axial position with the L–Ga–O bond angle to the opposite, axial alkoxide group ranging from 148.43(3)–151.17(5)°. This large deviation from 180° is due to the geometry of the ligand and the constraints of the internal O–Ga–O angle (range from 73.70(4)–77.27(4)°) in the Ga_2O_2 ring. The sum of the bond angles in the equatorial plane of **1**–**4** are close to 360°, which is a measure of the planarity of the equatorial groups. The equatorial Ga–O bond lengths in **1**–**4** are significantly shorter than the axial Ga–O bond distances (Table 2). The Ga–L distances in **1**–**4** range from 2.3727(11)–2.6266(10) Å and can be attributed to L → Ga dative bonding. The aminoalkoxide ligand in compound **4** possesses two donor (NMe_2) groups but only one coordinates to the gallium atom, such that the structure adopted is similar to **1**–**3**. The room temperature ^1H and ^{13}C NMR spectra of **4** are simple and show that the dimeric structure of the compound (Fig. 4) is fluxional under these conditions. Thus, the ^1H NMR of **4** only has one sharp singlet for the two distinct NMe_2 groups. In the related indium complex $[Me_2In(OCH(CH_2NMe_2)_2)]_2$ incorporating the same aminoalkoxide ligand, the indium atom is six-coordinate since both NMe_2 groups coordinate to the larger indium atom [19]. Some related methylalkoxogallanes, such as $[Me_2Ga(OCH_2CH(R)NMe_2)]_2$ (R = ^{i}Pr, Bz, Et) have been previously reported with comparable bond lengths and angles to **1**–**4** [26–28].

3.2. Chemical vapor deposition studies

3.2.1. Low pressure chemical vapor deposition

Low pressure chemical vapor deposition (LPCVD) of compounds **2** and **4** were investigated, the details of which are described in Section 2 [29]. These compounds were

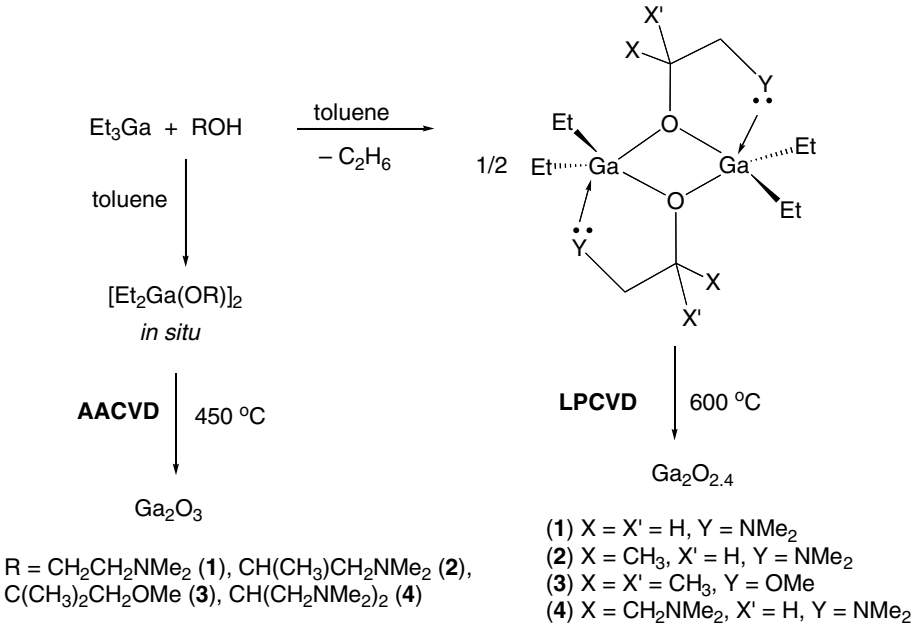

Scheme 1. Solution phase and CVD reactions of Et_3Ga and donor-functionalized alcohols.

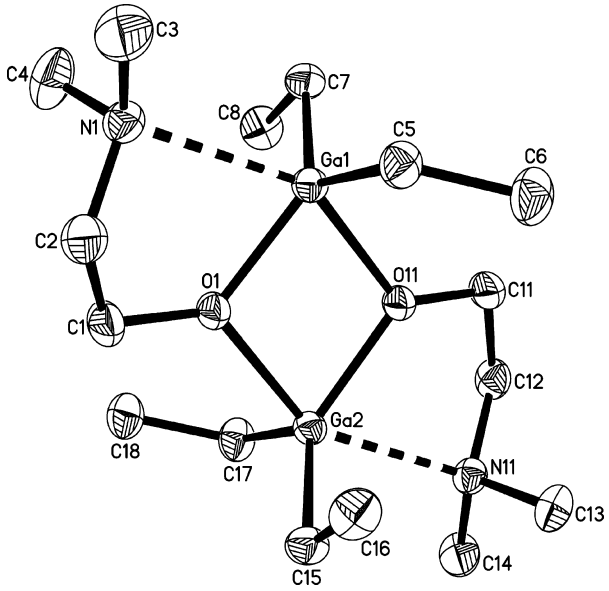

Fig. 1. Crystal structure of $[Et_2Ga(OCH_2CH_2NMe_2)]_2$ (**1**) with thermal ellipsoids shown at the 50% probability level (hydrogen atoms omitted for clarity).

selected on the basis of thermogravimetric analysis (TGA) under N_2, which showed that at 600 °C, compounds **2** and **4** gave the best deposition characteristics. Both **2** and **4** deposited light grey films on glass and quartz substrates at 600 °C. The films produced were analyzed by energy dispersive analysis of X-rays (EDAX), scanning electron microscopy (SEM), X-ray photoelectron spectroscopy (XPS), Raman and UV–Vis measurements. X-ray diffraction patterns for the films deposited from **2** and **4** indicated that they were amorphous, as expected for the deposition of gallium oxide at temperatures below 700 °C [14–16]. EDAX analysis and XPS revealed some carbon contamination (~10%) was present in the resulting films, which have a Ga:O ratio of 1:1.2. It is likely that the insufficient oxygen content in the precursor results in an oxygen deficiency (for Ga_2O_3) in the resulting films. However, XPS revealed binding energy shifts of 532.6 eV for O 1s and 1118.3 eV for Ga $2p_{3/2}$ for films grown from **4**. These binding energy shifts are in agreement with previous literature values for Ga_2O_3 [30]. Therefore, it is likely that Ga_2O_3 films have been formed but due to carbon contamination the ratio of Ga:O is not 1:1.5.

Scanning electron microscopy analysis of the film deposited from **2** at 600 °C showed a Volmer–Weber type island growth mechanism with spherical particles of 400 nm in size (Fig. 5a). The film produced from **4** showed a different morphology with particle sizes of 1 μm in diameter (Fig. 5b). All the films were investigated using Raman microscopy. In all cases no Raman scattering was observed and it is thought that gallium oxide is a poor Raman scatterer. However, Raman spectroscopy indicated the absence of graphitic carbon in the films. Conducting a Tauc plot [31] of the UV/visible data indicated that the films had a indirect band gap of 4.3 eV, comparable to other values for Ga_2O_3 of 4.2–4.9 eV [13,18,32].

3.2.2. Aerosol assisted chemical vapor deposition

The films grown from **2** and **4** *via* low pressure CVD were oxygen deficient, probably due to the low oxygen content in the precursor. Therefore, the AACVD reaction of Et_3Ga and excess ROH was investigated in an attempt to deposit higher purity gallium oxide films – the presence

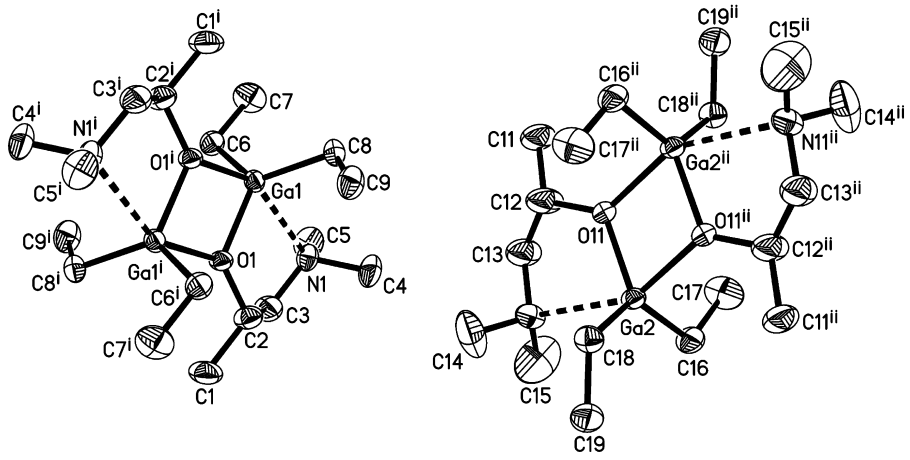

Fig. 2. Crystal structure of $[Et_2Ga(OCH(CH_3)CH_2NMe_2)]_2$ (**2**) with thermal ellipsoids shown at the 50% probability level (hydrogen atoms omitted for clarity). Symmetry codes: (i) $-x+1, -y+2, -z+1$ and (ii) $-x, -y+1, -z+2$.

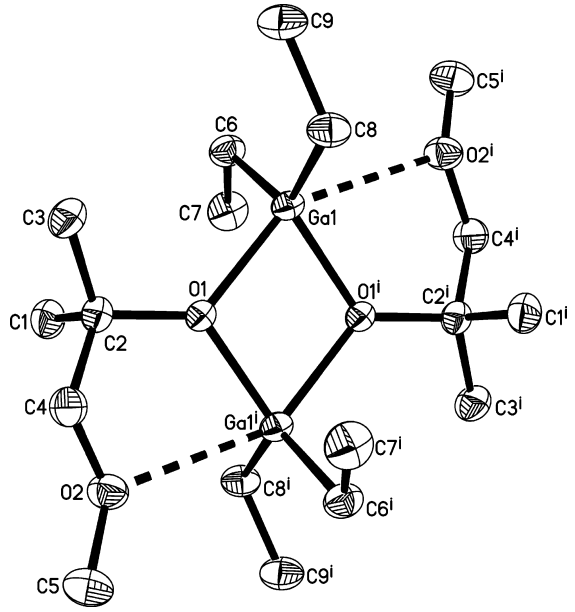

Fig. 3. Crystal structure of $[Et_2Ga(OC(CH_3)_2CH_2OMe)]_2$ (**3**) with thermal ellipsoids shown at the 50% probability level (hydrogen atoms omitted for clarity). Symmetry code: (i) $-x, -y+1, -z+1$.

of excess alcohol should reduce the oxygen deficiency. Transparent, unreflective films were deposited on glass from the dual-source AACVD reaction of Et_3Ga and ROH ($R = CH_2CH_2NMe_2$, $CH(CH_3)CH_2NMe_2$, $C(CH_3)_2$-CH_2OMe, $CH(CH_2NMe_2)_2$) at 450 °C (Scheme 1). The reaction of Et_3Ga and excess ROH in toluene was assumed to generate *in situ* the diethylalkoxogallane, $[Et_2Ga(OR)]_2$ (see above).

The films deposited displayed deposition localized mainly towards the leading edge of the substrate. This is a feature of fast growth kinetics and suggests that the reaction at the surface is mass transport limited. The films were adherent to the substrate, passing the Scotch Tape test but were readily scratched by a brass or stainless steel stylus. X-ray diffraction patterns for the films indicated that they were amorphous, as expected for the deposition of gallium oxide at these temperatures (<700 °C) [13–16].

The gallium oxide films were characterized using a range of techniques. WDX (wavelength dispersive analysis of X-ray) showed the films to have a gallium to oxygen ratio close to the expected 1:1.5 for Ga_2O_3 (Table 3). Furthermore, WDX indicated that there is little carbon contamination present in the resulting films (<0.1 at.%). All the films were investigated using Raman microscopy, but no Raman scattering was observed as expected. However, Raman spectroscopy indicated the absence of graphitic carbon in the films.

XPS of selected gallium oxide films show binding energy shifts for Ga $2p_{1/2}$, which are in close agreement with literature values previously reported for Ga_2O_3 (Table 3) [30]. XPS also showed a shift at 529.8 eV for the O 1s peak, which is in agreement with literature value of 530.5 eV for O 1s in Ga_2O_3 [30]. No evidence for carbon or nitrogen (for films grown from $HOCH_2CH_2NMe_2$, $HOCH(CH_3)$-CH_2NMe_2 and $HOCH(CH_2NMe_2)_2$) contamination was seen to the detection limits of the instrument.

The film morphology was studied using SEM, which indicated that deposition occurred via an island growth mechanism with particles of size 100 nm in diameter, as shown in Fig. 6a. Annealing the films in air at 600 °C resulted in a different morphology, with typical particle sizes of 1 μm and rods of about 10 μm (Fig. 6b and c). The films were approximately 300–400 nm thick, determined using cross-sectional SEM.

The optical properties of the films were studied by transmission, reflectance and UV/visible measurements between 300 and 2500 nm. All films showed a slight shift in the adsorption edge towards the visible relative to a plain glass substrate. The gallium oxide films displayed minimal reflectivity (5–10%) and high transmission (80–90%). Conducting a Tauc plot [31] of the UV/visible data indicated that the films had band gaps ranging from 4.5–4.7 eV. This is

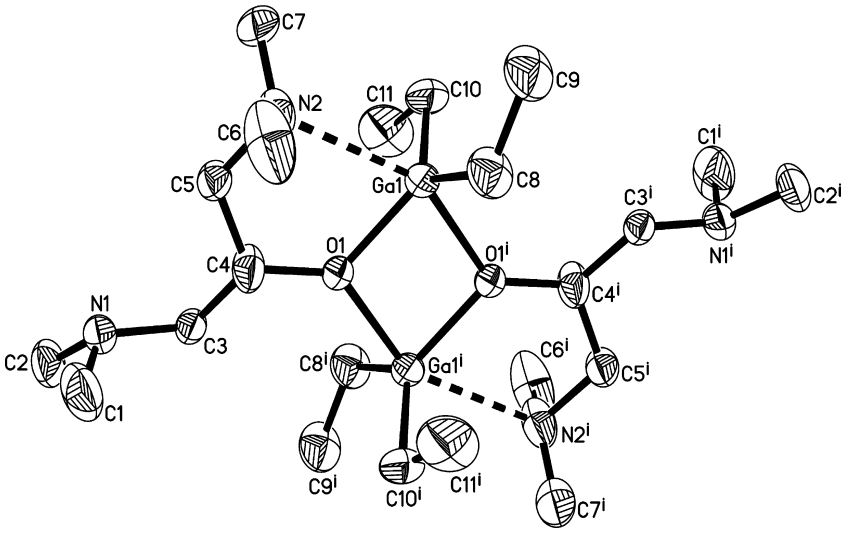

Fig. 4. Crystal structure of $[Et_2Ga(OCH(CH_2NMe)_2)_2]_2$ (**4**) with thermal ellipsoids shown at the 50% probability level (minor component and hydrogen atoms omitted for clarity). Symmetry code: (i) $-x+1, -y+1, -z+1$.

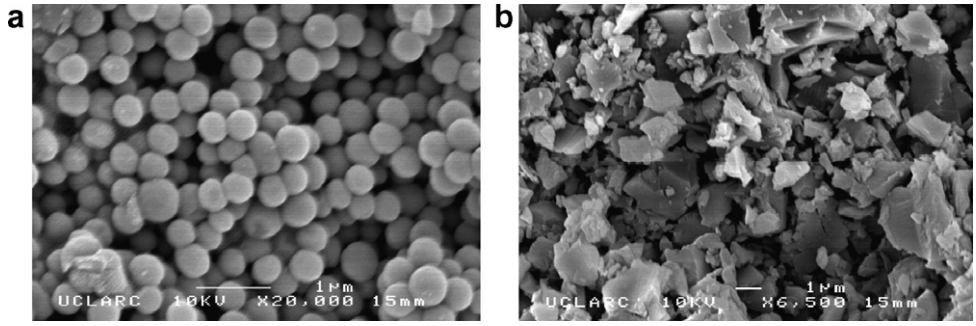

Fig. 5. SEM images for gallium oxide films deposited from (a) $[Et_2Ga(OCH(CH_3)CH_2NMe_2)]_2$ (**2**) and (b) $[Et_2Ga(OCH(CH_2NMe_2)_2)]_2$ (**4**).

Table 3
Analytical data for the deposition of Ga_2O_3 thin films by AACVD

Oxygen precursor	Ga:O ratio from WDX	XPS – Ga $2p_{1/2}$ binding energy shifts (eV)
$HOCH_2CH_2NMe_2$	1:1.5	1118.2
$HOCH(CH_3)CH_2NMe_2$	1:1.4	1118.4
$HOC(CH_3)_2CH_2OMe$	1:1.5	–
$HOCH(CH_2NMe_2)_2$	1:1.5	1119.2

in agreement with values previously reported [13,18,32]. The films were shown to have contact angles for water droplets of 24°, suggesting that the films are hydrophilic. However, the contact angles for these films did not change upon photo-irradiation suggesting that this low contact angle is not due to some form of photo-induced hydrophilicity. The porosity of the films could be responsible for this hydrophilic character.

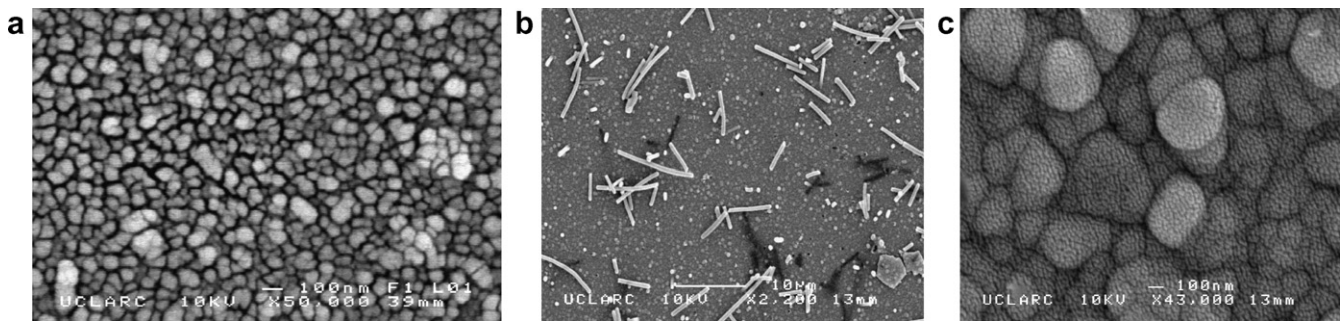

Fig. 6. SEM images for gallium oxide films deposited from the AACVD reaction of Et_3Ga and (a) $HOCH_2CH_2NMe_2$ (b) $HOCH_2CH_2NMe_2$ (post-annealing) and (c) $HOCH(CH_2NMe_2)_2$ at 450 °C.

The successful formation of Ga_2O_3 thin films from the *in situ* AACVD reaction of Et_3Ga and ROH indicates that there is no need to prepare, isolate and purify a single-source precursor. Compounds **1**–**4** were prepared from the 1:1 reaction of Et_3Ga and ROH at room temperature. However, for the AACVD experiments, although the mixture was stirred at the same temperature, the proportions of Et_3Ga to ROH were 1:6. Solution phase reactions between Et_3Ga and six equivalents of ROH at room temperature have been carried out but in all cases only diethylalkoxogallanes, $[Et_2Ga(\mu\text{-}OR)]_2$ (**1**–**4**), were isolated [33]. There was no evidence for the formation of ethyldialkoxogallanes $[EtGa(OR)_2]$ or gallium tris(alkoxides) $[Ga(OR)_3]_n$. Further reaction of $[Et_2Ga(\mu\text{-}OR)]_2$ with excess alcohol to yield the ethyldialkoxogallanes [EtGa- $(OR)_2$], is unlikely since the AACVD bubbler is maintained at room temperature and not heated to the temperatures necessary for further ethane elimination [17].

Amorphous Ga_2O_3 films were obtained from the AACVD reaction of Et_3Ga and ROH, which were superior to those deposited by low pressure CVD. Therefore, the use of excess alcohol led to stoichiometric Ga_2O_3 films with low levels of carbon contamination. The mechanism for the deposition process was not investigated. However, it is assumed to proceed *via* decomposition processes reported previously for related systems [34]. The ethyl and R group from $[Et_2Ga(\mu\text{-}OR)]_2$ are probably eliminated *via* β-hydride elimination when these complexes are pyrolyzed on or near the surface. The result of this would be the formation of intramolecular Ga–O bonds leading eventually to growth of Ga_2O_3.

4. Conclusions

Structural studies of the diethylalkoxogallanes, $[Et_2Ga(\mu\text{-}OR)]_2$ (**1**, R = $CH_2CH_2NMe_2$; **2**, R = $CH(CH_3)CH_2NMe_2$; **3**, $C(CH_3)_2CH_2OMe$; **4**, R = $CH(CH_2NMe_2)_2$) have shown that these compounds adopt dimeric structures with a planar Ga_2O_2 ring, and each gallium atom coordinated in a distorted trigonal bipyramidal geometry. Low pressure CVD of **2** and **4** resulted in the formation of oxygen deficient Ga_2O_3 thin films on glass. However, higher purity films of Ga_2O_3 can be grown from Et_3Ga and ROH (R = $CH_2CH_2NMe_2$, $CH(CH_3)CH_2NMe_2$, $C(CH_3)_2CH_2OMe$, $CH(CH_2NMe_2)_2$) under AACVD conditions. This represents the first deposition of Ga_2O_3 by AACVD using alkylgallium reagents [35]. Furthermore, the *in situ* reaction of Et_3Ga and ROH eliminates the need for the synthesis, isolation and purification of a single-source gallium alkoxide precursor.

Acknowledgements

EPSRC are thanked for a studentship (SB) and the MAPS faculty UCL for a research fund (CJC).

Appendix A. Supplementary material

CCDC 671230, 671231, 671232 and 671233 contain the supplementary crystallographic data for complexes **1**, **2**, **3** and **4**. These data can be obtained free of charge from The Cambridge Crystallographic Data Centre via www.ccdc.cam.ac.uk/data_request/cif. Supplementary data associated with this article can be found, in the online version, at doi:10.1016/j.jorganchem.2008.01.042.

References

[1] M. Fleischer, L. Höllbauer, H. Meixner, Sens. Actuators B 18–19 (1994) 119–124.
[2] M. Ogita, S. Yuasa, K. Kobayashi, Y. Yamada, Y. Nakanishi, Y. Hatanaka, Appl. Surf. Sci. 212–213 (2003) 397–401.
[3] Y. Li, A. Trinchi, W. Wlodarski, K. Galatsis, K. Kalantar-Zadeh, Sens. Actuators B 93 (2003) 431–434.
[4] M. Ogita, N. Saika, Y. Nakanishi, Y. Hatanaka, Appl. Surf. Sci. 142 (1999) 188–191.
[5] T. Schwebel, M. Fleischer, H. Meixner, C.-D. Kohl, Sens. Actuators B 49 (1998) 46.
[6] M. Fleischer, H. Meixner, Sens. Actuators B 26–27 (1995) 81.
[7] J. Passlack, Appl. Phys. 77 (1995) 686.
[8] T. Miyata, T. Nakatkani, T. Minami, Thin Solid Films 373 (2000) 145.
[9] J. Hao, M.J. Cocivera, Phys. D: Appl. Phys. 35 (2002) 433.
[10] L. Binet, D.J. Gourier, Phys. Chem. Solids 59 (1998) 1241.
[11] N.C. Oldham, C.M. Garland, T.C. McGill, J. Vac. Sci. Technol. A 20 (2002) 809.
[12] A. Oritz, J.C. Alonso, E. Andrade, C.J. Urbiola, Electrochem. Soc. 148 (2001) F26.
[13] R. Binions, C.J. Carmalt, I.P. Parkin, K.F.E. Pratt, G.A. Shaw, Chem. Mater. 16 (2004) 2489–2493.
[14] M. Valet, D.M. Hoffman, Chem. Mater. 13 (2001) 2135–2143.
[15] G.A. Battiston, R. Gerbasi, M. Porchia, R. Bertoncello, F. Caccavale, Thin Solid Films 279 (1996) 115–118.
[16] L.A. Mîinea, S. Suh, S.G. Bott, J.-R. Liu, W.-K. Chu, D.M. Hoffman, J. Mater. Chem. 9 (1999) 929–935.
[17] S. Basharat, W. Betchley, C.J. Carmalt, S. Barnett, D.A. Tocher, H.O. Davies, Organometallics 26 (2007) 403–407.
[18] S. Basharat, C.J. Carmalt, S.J. King, E.S. Peters, D.A. Tocher, Dalton Trans. (2004) 3475–3480.
[19] S. Basharat, C.J. Carmalt, S.A. Barnett, D.A. Tocher, H.O. Davies, Inorg. Chem. 46 (2007) 9473–9480.
[20] C.J. Carmalt, S.J. King, Coord. Chem. Rev. 250 (2006) 682.
[21] L.G. Hubert-Pfalzgraf, Inorg. Chem. Commun. 6 (2003) 102–120.
[22] Area Detector Control and Data Integration and Reduction Software, Bruker AXS, Madison, MI, USA, 2001.
[23] G.M. Sheldrick, SADABS, University of Göttingen, Germany, 1997.
[24] G.M. Sheldrick, SHELXS-97, University of Göttingen, Germany, 1997.
[25] G.M. Sheldrick, SHELXL-97, University of Göttingen, Germany, 1997.
[26] H. Schumann, S. Wernik, B.C. Wassermann, F. Girgsdies, J. Organomet. Chem. 621 (2001) 317–326.
[27] K.-H. Thiele, E. Hecht, T. Gelbrich, U. Dümichen, J. Organomet. Chem. 540 (1997) 89–94.
[28] H. Schumann, S. Dechert, F. Girgsdies, B. Heymer, M. Hummert, J.Y. Hyeon, J. Kaufmann, S. Schutte, S. Wernik, B.C. Wassermann, Z. Anorg. Allg. Chem. 632 (2006) 251–263.
[29] C.J. Carmalt, S.A. O'Neill, I.P. Parkin, E.S. Peters, J. Mater. Chem. 14 (2004) 830–834.
[30] D. Briggs, M.P. Seah (Eds.), Practical surface analysis, second ed., Volume Auger and X-ray Photoelectron Spectroscopy, Wiley, New York, 1990.

[31] J. Tauc (Ed.), in: Proceedings of the International School of Physics, Enrico Fermi, Course XXXIV, The Optical Properties of Solids, 1966.
[32] Z. Hajanal, J. Miro, G. Kiss, F. Reti, P. Deak, R.C. Herndon, J.M. Kuperberg, J. Appl. Phys. 86 (1999) 3792.
[33] S. Basharat, Ph.D. Thesis, University of London, 2007.
[34] C.J. Carmalt, S. Basharat, in: D. O'Hare (Ed.), Comprehensive Organometallic Chemistry, vol. 12, 2007, pp. 1–34.
[35] S. Basharat, C.J. Carmalt, R. Binions, R. Palgrave, I.P. Parkin, Dalton Trans. (2008) 591–595.